

Continuous Heating and Cyclic Heating for Composite Materials Containing PA2200 and Ceramic Additives (Al_2O_3 , MgO and Nanoclay) Monitoring System

Meraj Danish

Department of Mechanical Engineering, Maharshi University of Information Technology, Lucknow, India

ABSTRACT

In this harsh competition, additive manufacturing (AM) is an incredible breakthrough for aerospace, automobile and tooling industries. It can transform a computer-aided-design (CAD) into 3D component without tools or human intervention. Selective Laser Sintering (SLS) is an AM technique that utilizes high power laser to sinter tiny particles of a polymer powder into a solid object based on 3D model data. This work focuses on improving material optimization for the SLS process and establishing the best fabrication settings for developing products with superior attributes. By combining a commercially-available SLS materials like: PA2200 (polyamide) with ceramic additives (e.g., Al_2O_3 , MgO and Nanoclay), new composite materials have been produced. It is shown that these composite materials are capable to produce sintered specimens that have superior mechanical and flammability properties than that of pure PA2200.

Keywords: Selective Laser Sintering, polyamide, Mechanical Properties, Flammability

1. Introduction

Selective Laser Sintering (SLS) is an (AM) technology that can produce complex component geometry directly from 3D CAD software [1]. SLS builds parts from powder. Sintered components are produced when an infrared (IR) laser beam's heat overcomes the surface tension of particles, fusing them together [2, 3]. Two feed cartridges distribute powder over the construction area with a roller so that the next layer may be applied. This continuous until the part is produced. Through the use of a low melting point temperature binder, the SLS method is being employed to synthesize a variety of materials with varied properties as well as triturated substance to generate a geometrically precise sintered object. According to Madea and Childs, the SLS process has the capacity to adapt to a variety of materials [4]. SLS is among the most crucial prototype methods. To evade probable fire of the powder quantifiable particles, the entire polymer processing method is carried out in a heated hollow filled with inert fume. The powder layer is scanned and heated by the laser beam's thermal energy, causing shared sintering of the physical particles. The stage is dropped for the width of one coat, allowing a fresh powder layer to be laid. The new layer is perused, modified to the next higher cross-section, and adhered to the old one. SLS made prototypes are increasingly being employed as functioning parts with good mechanical qualities. The precision of the CAD prototypical, the technique of sheet cutting, machine determination, ray balance, coating width, material reduction, optical maser speediness, laser control, energy compactness, working improper temperature and hatching coldness are all elements that influence this need. Thus, AM refers to the layer-by-layer fabrication of three-dimensional physical models directly from CAD without any cutters, tools of fixtures specific to the object geometry [5, 6]. Objects of any kind of geometric (direct assemblies, conformal, custom, complex) or material (any variety-poly/metal/ceramic, non-equilibrium, gradient-mono/composite/gradient, porous/lattice, soft/hard) intricacy can be produced. Federico Lupone [2], utilized information

from a 3D model, the SLS process melts just the areas of a polymer powder bed that are needed to create a final product. Then, a layer-by-layer method is used to acquire the complicated geometric components.

Khalid Mutashar Abed [3] reported that SLS may be used with a broad variety of materials, giving researchers a new avenue to explore in the field of AM or Solid Freeform Fabrication (SFF). In order to improve the quality and mechanical qualities of the components mentioned, various studies have been conducted using SLS technique on materials such as polymer metal composite ceramics and sand.

According to Lu Pan [4], selective laser melting (SLM) has emerged as a leading technology for metal AM. SLM is used to create 3D pieces in order to establish corrections between mechanical qualities, microstructure, and process parameters. SLM process's success in reducing grain size, and its mechanical qualities.

Both SLS and SLM, is a powder-based additive manufacturing process that allows the production of functional 3D parts directly from a CAD-model. During the process, successive layers of metal powder particles are molten and consolidated on the top of each other by the energy of a high intensity laser beam. Consequently, almost fully dense parts without need for any post-processing other than surface finishing are produced. Customized medical parts, tooling inserts with inserts with conformal cooling channels and functional components with high geometrical complexity are good examples to reveal the scope of the application areas of this process [7, 8]. SLS automatically fuses powdered industrial materials together using a high-powdered laser, SLM fuses powdered materials together by heating them until they reach a melting point.

Fig. 1 shows a schematic example of SLS system. Commercial machines differ for example in the way the powder is deposited (roller or scraper), the atmosphere, and in the type of laser they use (Fiber, CO_2 , or Nd: YAG laser).

*Corresponding author: mech.mdmdanish@gmail.com

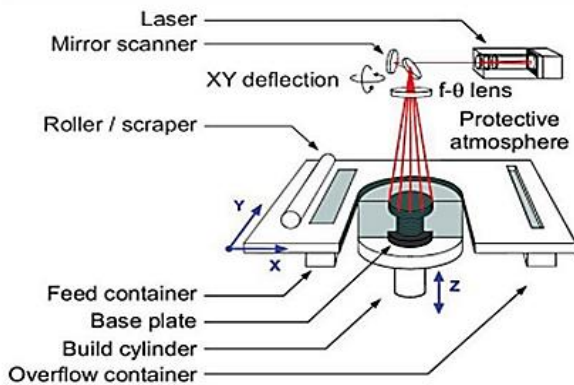


Fig. 1: A schematic view of the SLS/SLM process

Laser processing of materials is generally accompanied with high cooling rates due to the short interaction time and high thermal gradients. The high cooling rates during SLS/SLM may result in the formation of non-equilibrium phases, quasi-crystalline phases and new crystal phases with extended composite ranges. Finer structures may be observed in the microstructure at sufficiently high cooling rates compared to the conventional manufacturing methods. Moreover, during the SLS/SLM process, gas bubbles and oxide inclusions can become entrapped in the material during solidification due to various causes such as decrease in the solubility of the dissolved elements in the melt pool during cooling and solidification, chemical reaction or trapped gas. Therefore, the mechanical and material properties obtained after SLM may be different than the properties of materials produced by conventional production techniques [9].

2. Materials and Methods

2.1 Materials in SLS

SLS can process almost any substance as long as it's in dry powder and the powder particles ignite or sinter when heated. The bulk of materials falls within this category. Powder particles with limited fusing or sintering abilities can be laser sintered by adding a substitute binder material (typically a polymer) to the basic powder. Once the entire piece has been sintered, the sacrificial binder may be removed depending on the "green" area (in which the metal particles are bounded together by polymer-polymer bonds) in a thermal furnace. The green part is usually porous, has low mechanical properties and need to be post-processed. The use of a sacrificial binder allows for the expansion of the pellet of laser sinterable materials. Laser sintering stands out among fast prototyping processes with its extensive material compatibility, surpassing other sinterable materials and techniques. It enables rapid production and processing of a wide range of materials, making it a versatile and efficient method for fast prototyping applications, however, the range of materials (powders) that can be laser sintering without a fatal binder is rather extensive [10]. In SLS, polymer dry powders are the initial and are yet the most extensively used product.

Parts made from amorphous polymers, such as polycarbonate (PC) powders, provide excellent dimensional precision, feature determination, and shallow quality (contingent on the ounce size). They are, however, partly cemented. As a result, these components are only suitable for situations where part strength and longevity are not required. SLS masters are commonly used in the production of silicone rubber and cast epoxy moulds.

Semi-crystalline polymers, such as nylons (polyamide (PA)), can be sintered to generate completely dense components with mechanical properties equivalent to injection moulded ones. The total shrinkage of these semi-crystalline polymers throughout the SLS process is around 4%, hindering the manufacture of accurate components. The mechanical properties of these nylon-based components make them perfect for high-strength functional prototypes [11]. Even though amorphous powders may still generate higher resolutions and smoother surfaces, new nylon powder grades (such as Duraform PA12) provide resolution and surface roughness that is comparable to PC, making PA ideal for casting silicone rubber and epoxy moulds respectively.

2.2 Working Principle of Additive Manufacturing

In contrast to subtractive manufacturing methods, additive manufacturing is described by ASTM F2792 – 12A as "the process of combining materials to produce items from 3-D model data, generally layer upon layer" [12]. To further understand how the AM process works, the product's CAD model is originally developed in modelling software with the help of the product's requirements. After CAD model is created, it is sectioned along parallel planes that have the same width as the individual layers. The resulting slices have sharp, squared-off edges, much like the staircase effect. These once 3D models are now reduced to the smaller 2D slices. It seems like a difficult 3D issue has been simplified into a set of 2D planes. The geometric 3D model is tiled into a compact 2D file called an STL file before being sent out. Tessellation is the process of approximating the surfaces of a CAD model with a grid of triangles, with each triangle's surface normal and vertex coordinates being recorded.

2.3 Methodology

Sample of composite materials containing PA2200 and one of three ceramic additives (Al_2O_3 , MgO and Nanoclay) were heated in an oven simulating the SLS process under conditions designed to mimic those of the SLS process, the oven was kept at a specific temperature (211°C) for a range of times, and the powders were kept from oxidizing (yellowing) by a constant supply of nitrogen. Because the powder in the left and right cartridges can only be exposed to a maximum of 100°C during SLS process, and the powder in the bed section can only be subjected to a maximum of 180°C , samples of the composite materials were heated to both of these temperatures. Composite material samples were stored at room temperature and then in the refrigerator for 25, 50, 75, and 100 hours. There are two ways to heat samples of shaped composite materials, (i) continuous heating and (ii) cyclic heating. The first (continuous heating method is used to

simulate the SLS process for a single build, while the second (cyclic heating) method simulates the SLS process for multiple builds by removing the composite materials samples from the oven, allowing them to cool to room temperature, and then re-heating them. The impact of time and temperature on the powder characteristics was investigated by testing and analyzing sample composite materials with a particle size of 75 to 100 μm , in its natural state, the material is semi-crystalline. The flammability grade value with respect to Nanoclay wt.% in PA2200 shown in Table 1.

For constructing components in SLS process, we often

Table 1 Flammability grade value with respect to nanoclay wt% in PA2200

| Sr. No | Wt.% Nanoclay | Flammability Grade | Remark 1 | Remark 2 | Remark 3 |
|--------|---------------|--------------------|---|---|---|
| 1 | 0 | V ₂ | Flame restated in 30 second after either application of test flame. | Time may not exceed 250 seconds for the ten flame applications for each set of 5 specimens. | The specimens can drip flaming particles. |
| 2 | 5 | V ₂ | Flame restated in 30 second after either application of test flame. | Time may not exceed 250 seconds for the ten flame applications for each set of 5 specimens. | The specimens can drip flaming particles. |
| 3 | 10 | V ₂ | Flame restated in 30 second after either application of test flame. | Time may not exceed 250 seconds for the ten flame applications for each set of 5 specimens. | The specimens can drip flaming particles. |
| 4 | 15 | V ₁ | Flame retards in 30 seconds after either application of test flame. | Time may not exceed 250 seconds for the ten flame applications for each set of 5 specimens. | The specimens may not drip flaming particles. |

2.4 Details of material

Figure 2 is made from Polyamide Duraform powder. The previously used powder has qualities that differ from virgin powder after going through a heating cycle. The material utilized had been renewed, and the mixing ratio was 70% used powder and 30% virgin powder [13]. Because using more fresh powder causes the product to curl, only 30% fresh powder may be utilized to make components.

2.5 SLS test parts layout

These five pieces are manufactured at a process station (Vanguard HS) in this SLS setup, as depicted (Figure 2–Figure 6). As illustrated, the pieces are placed in the construction. The central part is exactly in the middle of the construct, with the other parts at similar distances from the center, i.e., the origin of additional parts is 35 mm out from the shape's center. It was known quality, based on sintering presentation involvement, that pieces were put in the same plane/build sinter with minimum delay. As a result, additional tests, i.e., the fabrication of other pieces throughout a similar variety of parameters as the rectangular blocks, are carried out to give samples for the various measurements.

The percentage by weight of fillers in PA2200 corresponds to the flammability grade rating shown in Table 2. The composite materials were heated at 100°C and 180°C for 25, 50, 75 and 100 hours to determine the best values for the process parameters. DSC analysis was performed on the heat-treated samples (ISO 11357–6, 2008). The DSC curve shows that the glass transition, recrystallization, and melting point of PA2200 are hardly impacted by loading with different concentrations of three different additives (Al₂O₃, MgO and Nanoclay) (see Figure 2, Figure 3, Figure 4, Figure 5, Figure 6). The following figures shows the connection between T_g,

utilize a blend of compliance with the specifications. To obtain a good surface smoothness the procedure parameters employed for outline contact include lower laser control and skimming speed compared to shading exposure. It will deform if not allowed to cool in a controlled atmosphere for an extended period of time due to the outer environment's quick cooling. The component acquires large pressures as it cools fast. As a result, the part is permitted to cool for 4–5 hours inside the platform. Specification for constructing components, we often utilize a blend of new powder and previously used but unsintered powder.

T_c and T_m of composite materials as determined by analyzing the DSC data for the materials. Graph 1 displays the effects of temperature and time on the glass transition, transition temperature, and transition temperature of Silane–Montmorillonite (SMMT) Nanoclay/PA2200 composite, Graph 2 displays the effect of temperature and time on T_g of SMMT Nanoclay/PA2200 composite, Graph 3 displays the effect of temperature and time on T_c of SMMT Nanoclay/PA2200 composite, Graph 310 displays the effect of temperature and time on T_m of SMMT Nanoclay/PA. Theoretically, it has been postulated that the molecular weight is a common factor impacting T_g, T_c and T_m of the composite material. An increase in molecular weight is held accountable for an increase in T_g and T_m of the composite material, while a decrease in T_c of the composite material is held accountable. Furthermore, crystalline index (CI) is a key factor in obtaining a high-quality SLS sintered component [14]. By factoring in the percentage by weight of polymer in the composite, the crystalline index (CI) was determined using Equation;

$$CI = \frac{\Delta H_m}{\Delta H_f(1 - f)} \times 100$$

“Where ΔH_f is melting enthalpy for a theoretically 100 percent crystalline PA2200, which is 209.2 J/g and f is the mass fraction of the filler. The peak melting temperature T_m, peak crystalline temperature T_c, melting enthalpy ΔH_m and crystalline enthalpy ΔH_c were extracted from the DSC curves. The CI% value is calculated for PA2200 and mentioned composite materials using the equation. Melt Flow Index (MFI) is a crucial metric for gauging the quality of SLS fabricated components.

3. Measurements

3.1 Dimensional Accuracy

As illustrated in Figure 7 and Table 2, the dimensional accuracy of SLS specimens is indicated by error S_1 . For each worth, three capacities are taken and the normal value is obtained. The dimensional error S_1 represents the part's dimensional correctness and is defined as:

$$S_1 = \left[\frac{A_1 - A_0}{A_0} \right] \times 100$$

Where A_0 is the computer – generated design size and A_1 is the actual size unrushed using a vernier caliper. At this point in the sintering process, the material dimensions are stable. The sintering process has two stages, the first of which is the formation of the neck, and the second of which is the completion of the sintering process. The early sintering, stage so often occurs during heating and is characterized by the rapid expansion of the interparticle neck. As the neck grows, sinter mass is transferred along with it. There is no shrinking at this stage because the sinter mass does not lose porosity throughout this process.

3.2 Melt Flow Index (MFI)

Manually calculating the MFI from the known sample to Mass and measurement time yields values expressed in g/10 min; The formula used to determine MFI is

$$MFI(T_m) = \frac{600m}{t}$$

MFI is significant in the combination of Nanoclay and PA2200 materials as it evaluates their flowability and processability, ensuring efficient and consistent SLS outcomes.

3.3 Melting Temperature (T_m)

The melting temperature is reached when the polymers have accumulated enough thermal energy to begin chain motion freely enough to behave like a viscous liquid. The temperature has a significant effect on the viscosity of the molten polymer. Even more, when the temperature rises, the polymer's viscosity drops automatically:

$$\eta_0 = A \exp(\Delta E/RT)$$

3.4 Mechanical Properties

Mechanical Properties of specimens studied under ambient conditions: include tensile strength, elongation at break, and density. As illustrated specimens were examined using universal testing equipment.

4. Results and Discussion

4.1 Results

To enhance the flame retardant and mechanical properties of the sintered specimen and lower the cost of the Polyamide 12 through the addition of ceramic additives, a new composite material has been developed from ceramic additives (Al_2O_3 ,

MgO and Nanoclay) separately with Polyamide 12 (PA2200) (Al_2O_3 , MgO and Nanoclay).

For the purpose of controlling SLS parameters and obtaining consistent quality of fabricated SLS specimens, the thermal properties of composite materials of ceramic additives (Al_2O_3 , MgO and Nanoclay) filler and Polyamide 12 of the virgin powder have been studied at various filler percentages (ranging from 0% to 15% by weight).

In an effort to cut down on production time and material waste, researchers have investigated the feasibility of using a technique called pressure less casting to create specimens with qualities comparable to those of SLS components.

It is planned to implement a mechanism for adjusting the percentage of ceramic additions (Al_2O_3 , MgO and Nanoclay) filler in Polyamide 12. The use of virgin powder in the SLS system and the creation of a mechanism for regulating the quantity of virgin powder to be added to use powder have both been explored. Powder fitness and mechanical characteristics may be accurately predicted using the melt flow index (MFI), as shown by the correlation between the two [15, 16].

Additionally, a summary of the materials used in the SLS process is provided, and a methodology is developed for selecting the material to be used in the part fabrication on the SLS process based on the properties requirement of application for a fluorescent lamp holder product, by way of the value engineering method. For appropriate material selection and the manufacturing of high – quality components using the SLS process, the method shown in this demonstration has been demonstrated to be effective. The addition of Al_2O_3 , MgO and Nanoclay in polyamide 12 (PA12) can have various effects. Al_2O_3 and MgO can enhance the mechanical properties, such as strength and stiffness, while Nanoclay can improve thermal stability and barrier properties. These additives can enhance the overall performance and functionality of PA12–based materials.

4.2 Mechanical Properties

Table 3 lists the mechanical characteristics of the polyamide SLS sample. The tensile strength and extension at the disruption of these SLS samples are both quite low, according to estimated values. The fundamental reason for this is that these components have a low thickness and a large number of voids. Furthermore, the influence of layout on mechanical properties on various portions shows that mechanical characteristics decline as we advance down the Y-axis.

Figures 8 shows pictures of several samples collected using a metallurgical microscope. We can see that the powder particles are not tightly packed, and we can still clearly distinguish between them. Only adjacent particles link together, resulting in distinct pores in the components, which are visible from the sintered part/engulfed air bubble. These are feasible as a result of the evaluation of gases during the solidification process. Which leads to a reduction in the mechanical characteristics of certain sections.

4.3 Melt Flow Index

Metal Flow Index is a crucial metric for gauging the quality of SLS-fabricated components and determining whether to re-inject virgin powder with proper amount of reclaim (Chow and Ishak Mohd 2007). To find best settings for the SLS process, it is helpful to have a firm grasp of the thermal characteristics of composite material made up of PA12 plus one or more additives (Al₂O₃, MgO and Nanoclay). In addition, the thermal and physical characteristics of both sintered and unsintered powder are investigated in order to provide a system for regulating SLS parameters and ultimately for achieving reliable, high-quality SLS specimens throughout the fabrication process. Exposure of the unsintered

powder to high temperatures and long heating durations are the most influential elements in the ageing or degradation of composite material of three distinct additions (Al₂O₃, MgO and Nanoclay) with PA12 [17]. Graph 1 displays the melt flow index of the SMMT Nanoclay/PA2200 composite, Graph 2 displays that of the Aluminum Oxide / PA2200 composite, and Graph 3 displays that of the Magnesium Oxide / PA2200 composite. When comparing the effects of MFI on materials heated to 100°C for 0 – 100 hours against 180°C for 0 – 100 hours, the former has a smaller impact. At 180°C and during the first 25 hours, the MFI decreases the most, and the competition for the same temperature and time period causes the viscosity to rise quickly.

Table 2. Dimensional accuracy of SLS parts

| Sr. No. | Measurements | A ₀ | S ₁ % of Part 1 | S ₁ % of Part 2 | S ₁ % of Part 3 | S ₁ % of Part 4 | S ₁ % of Part 5 | |
|---------|-------------------|----------------|----------------------------|----------------------------|----------------------------|----------------------------|----------------------------|-------|
| 1 | Length of side | X | 30 | 0.25 | 0.264 | 0.258 | 0.254 | 0.265 |
| | | Y | 30 | 0.26 | 0.263 | 0.257 | 0.261 | 0.264 |
| 2 | Width of rib | X | 1 | 0.12 | 0.18 | 0.09 | 0.07 | 0.19 |
| | | Y | 1 | 0.12 | 0.19 | 0.06 | -0.03 | 0.19 |
| 3 | Thickness | Z | 3.75 | 0.33 | 0.333 | 0.333 | 0.336 | 0.370 |
| 4 | Circle at center | R ₁ | 1.5 | 0.073 | -0.04 | 0.113 | 0.133 | -0.14 |
| | | R ₂ | 1.5 | 0.086 | -0.033 | -0.02 | 0.186 | -0.03 |
| | | R ₃ | 1.5 | 0.060 | -0.006 | 0.106 | 0.146 | 0.12 |
| 5 | Thickness of base | Z | 1.25 | 0.416 | 0.448 | 0.464 | 0.456 | 0.528 |
| 6 | Average | S% | | 0.138 | 0.156 | 0.170 | 0.192 | 0.185 |

Table 3. Mechanical Properties of SLS Parts

| Sr. No. | Measurements | Values of Part 1 | Values of Part 2 | Values of Part 3 | Values of Part 4 | Values of Part 5 |
|---------|-------------------------|------------------|------------------|------------------|------------------|------------------|
| 1 | Tensile Strength (MPa) | 47.49 | 47.48 | 47.48 | 47.48 | 47.45 |
| 2 | Elongation at break (%) | 17.3 | 17.2 | 17.2 | 17.0 | 17.1 |
| 3 | Density (gm/cc) | 0.960 | 0.958 | 0.558 | 0.57 | 0.595 |

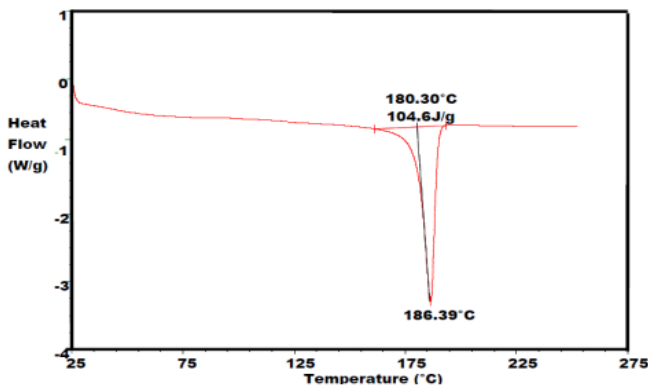


Figure 2: DSC of PA2200 (Non – heat treated)

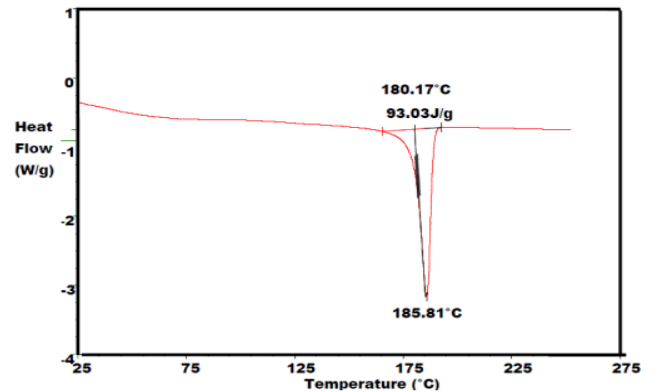


Figure 3: DSC of SMMT Nanoclay 5 wt.% / PA2200 composite (Non – heat treated)

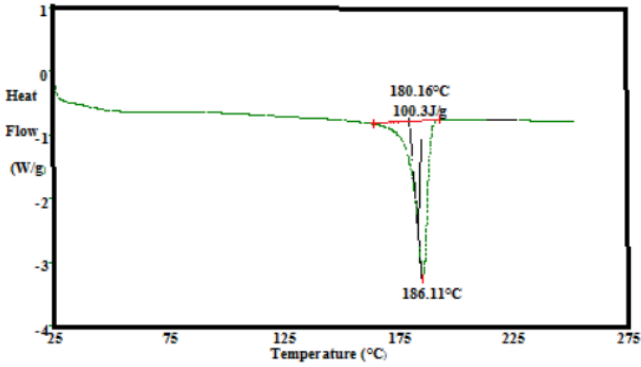
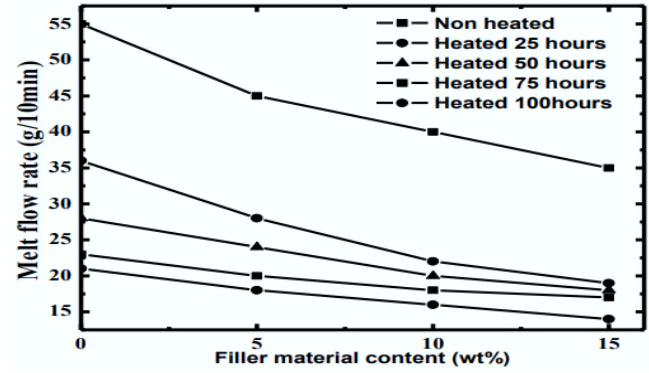


Figure 4: DSC of Aluminum Oxide 5 wt.% / PA2200 composite (Non – heat treated)



Graph 2: Melt Flow Index of Aluminum Oxide / PA2200 composite

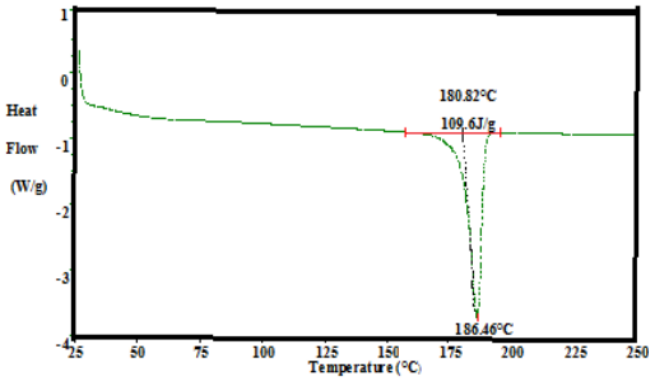
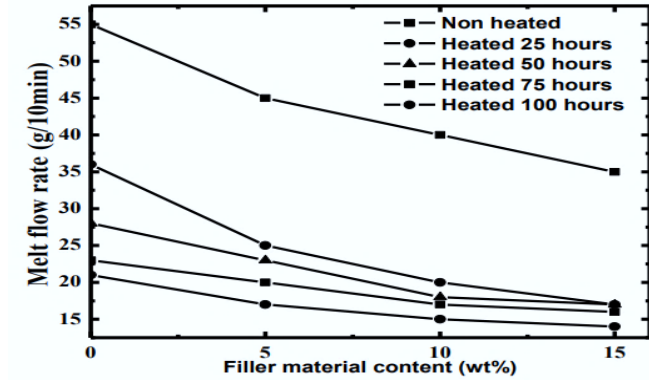


Figure 5: DSC of Aluminum Oxide 10 wt.% / PA2200 composite (Non – heat treated)



Graph 3: Melt Flow Index of Magnesium Oxide / PA2200 composite

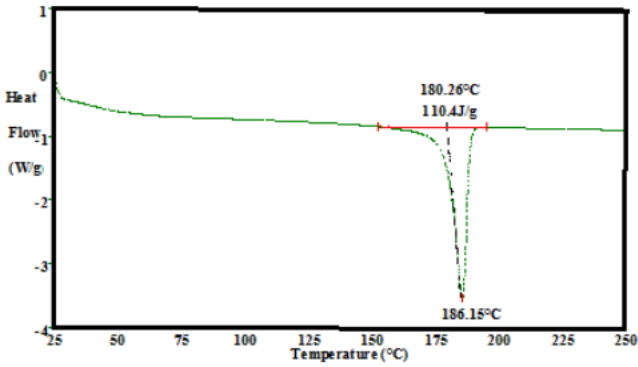
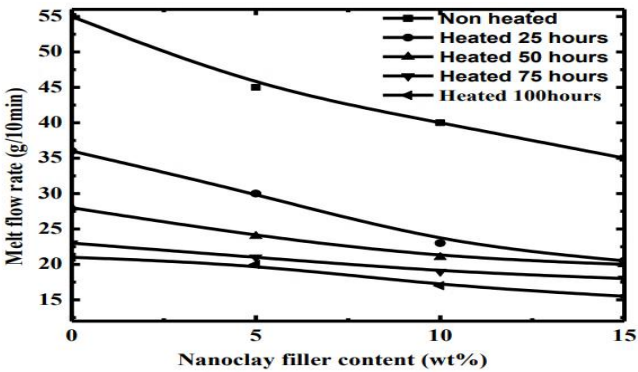


Figure 6: DSC of Magnesium Oxide 5 wt.% / PA2200 composite (Non-heat treated)



Graph 1: Melt Flow Index of SMMT Nanoclay/PA2200 composite

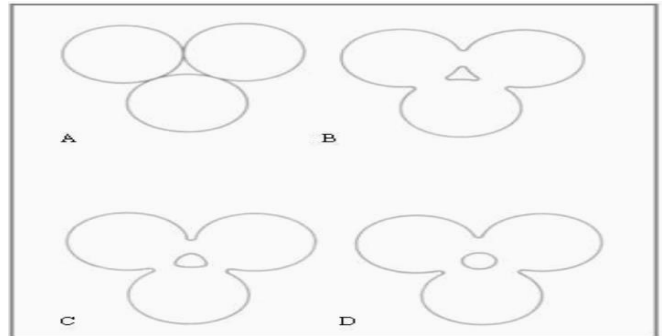


Figure 7: Three sphere sintering model (A) Original Point Contacts (B) Neck Growth (C) Pore Rounding

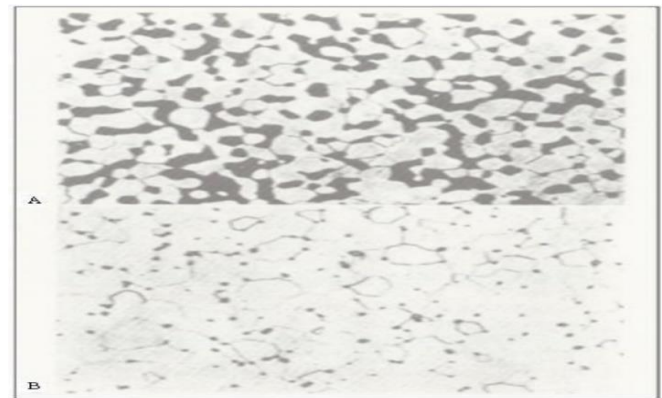


Figure 8: Photo micrographic illustration of change from interconnected to isolated porosity (A) Early phase with interconnected porosity (B) Later Phase with closed porosity

5. Conclusion

The fields in which additive manufacturing is used are expanding. Particularly relevant to the SLS technique. Improvements in the utilized material are necessary for the SLS method to become competitive and a good option for innovative applications (i.e., quick production). The goal of this study is to reduce the price of Polyamide 12 and significantly enhance the quality of SLS fabricated parts by first optimizing the selection of existing materials based on the properties required by applications, and then improving the properties of SLS materials by combining ceramic additive (Al_2O_3 , MgO and Nanoclay) with Polyamide 12 to form a new composite material (Al_2O_3 , MgO and Nanoclay).

Reference

- [1] M. Siming, S. Zhongxia, A. Shang, P. Zhang, C. Tang, Y. Huang, C.L.A. Leung, P.D. Lee, X. Zhang, and X. Wang, "Additive manufacturing enabled synergetic strengthening of bimodal reinforcing particles for aluminum matrix composites," *Additive Manufacturing Journal*, vol. 70, no. 3, pp. 103–117, May 2023.
- [2] F. Lupone, E. Padovano, F. Casamento, and C. Badini, "Process phenomena and material properties in selective laser sintering of polymers," *Materials Journal*, vol. 15, no. 1, pp. 1–37, Dec 2021.
- [3] K.M. Abed, "Investigation of properties of selective laser sintering of titanium alloy composite," *Journal of Mechanical Engineering Research and Development*, vol. 44, no. 9, pp. 34–44, May 2021.
- [4] P. Lu, Z.C. Lin, W. Liang, L. Tong, and L.X. Cheng, "Research on mechanical properties and microstructure by selective laser melting of 316L stainless steel," *Mater. Res. Express*, vol. 6, no. 12, pp. 60–80, April 2020.
- [5] N.A. Hamzah, N.A.A. Razak, M.S. Karim, and H. Gholizadeh, "A review of history of CAD/CAM system application in the production of transibial prosthetic socket in developing countries (from 1980 to 2019)," *Proceedings of the Institution of Mechanical Engineers, Part H: Journal of Engineering in Medicine*, vol. 235, no. 12, pp. 1359–1374, July 2021.
- [6] T. Kozior, C. Dopke, N. Grimmelsmann, I.J. Junger, and A. Ehrmann, "Influence of fabric pretreatment on adhesion of three-dimensional printed material on textile substrates," *Advances in Mechanical Engineering*, vol. 10, no. 2, pp. 1–8, Aug 2018.
- [7] J. Bochnia, and S. Blasiak, "Fractional relaxation model of materials obtained with selective laser sintering technology," *Rapid Prototyping Journal*, vol. 25, no. 1, pp. 76–86, Jan 2019.
- [8] S. Fafenrot, N. Grimmelsmann, M. Wortmann, and A. Ehrmann, "Three-dimensional (3D) printing of polymer-metal hybrid materials by fused deposition modeling," *Materials Journal*, vol. 10, no. 10, pp. 209–219, Oct 2017.
- [9] T. Kozior, and C. Kundera, "Evaluation of the influence of parameters of FDM technology on the selected mechanical properties of models," *Procedia Engineering*, vol. 192, no. 7, pp. 463–468, June 2017.
- [10] S. Adamczak, P. Zmarzly, T. Kozior, and D. Gogolewski, "Assessment of roundness and waviness deviations of elements produced by selective laser sintering technology," *23rd International Conference Engineering Mechanics*, pp. 70–73, May 2017.
- [11] E.O. Olakanmi, R.F. Cochrane, and K.W. Dalgarno, "A review on selective laser sintering/melting (SLS/SLM) of aluminum alloy powders: Processing, microstructure, and properties," *Progress in Materials Science*, vol. 74, pp. 401–477, Oct 2015.
- [12] C. Kundera, and T. Kozior, "Mechanical properties of models prepared by SLS technology," *AIP Conference Proceedings*, vol. 17, no. 2, pp. 1–12, Oct 2018.
- [13] A. Verma, S. Tyagi, and K. Yang, "Modeling and optimization of the direct metal laser sintering process," *Springer's International Journal of Advanced Manufacturing Technology*, vol. 77, no. 7, pp. 847–860, Oct 2014.
- [14] C. Kundera, and T. Kozior, "Elastic bellows prepared by selective laser sintering," *Applied Mechanics and Materials*, vol. 630, no. 17, pp. 318–325, Sep 2014.
- [15] G.V. Salmoria, J.L. Leite, L.F. Vieria, A.T.N. Pires, and C.R.M. Roesler, "Mechanical properties of PA6/PA12 blend specimens prepared by selective laser sintering," *Polymer Testing*, vol. 31, no. 3, pp. 411–416, May 2012.
- [16] K.A. Ghany, and S.F. Moustafa, "Comparison between the products of four rpm systems for metals," *Rapid Prototyping Journal*, vol. 12, no. 2, pp. 86–94, Mar 2006.
- [17] M. Badrossamay, and T.H.C. Childs, "Further studies in Selective Laser melting of Stainless and Tool Steel Powders," *International Journal of Machine Tools and Manufacture*, vol. 47, no. 5, pp. 779–784, April 2007.